Inhibition of the T790M Gatekeeper Mutant of the Epidermal Growth Factor Receptor by EXEL-7647

Steven B. Gendreau, Richard Ventura, Paul Keast, A. Douglas Laird, F. Michael Yakes, Wentao Zhang, Frauke Bentzien, Belinda Cancilla, Jeffery Lutman, Felix Chu, Lisa Jackman, Yongchang Shi, Peiwen Yu, Jing Wang, Dana T. Aftab, Christopher T. Jaeger, Stephanie M. Meyer, Anushka De Costa, Kelly Engell, Jason Chen, Jean-Francois Martini, and Alison H. Joly

Abstract

Purpose: Agents inhibiting the epidermal growth factor receptor (EGFR) have shown clinical benefit in a subset of non–small cell lung cancer patients expressing amplified or mutationally activated EGFR. However, responsive patients can relapse as a result of selection for *EGFR* gene mutations that confer resistance to ATP competitive EGFR inhibitors, such as erlotinib and gefitinib. We describe here the activity of EXEL-7647 (XL647), a novel spectrum-selective kinase inhibitor with potent activity against the EGF and vascular endothelial growth factor receptor tyrosine kinase families, against both wild-type (WT) and mutant EGFR *in vitro* and *in vivo*.

Experimental Design: The activity of EGFR inhibitors against WT and mutant EGFRs and their effect on downstream signal transduction was examined in cellular assays and *in vivo* using A431 and MDA-MB-231 (WT EGFR) and H1975 (L858R and T790M mutant EGFR) xenograft tumors.

Results: EXEL-7647 shows potent and long-lived inhibition of the WT EGFR *in vivo*. In addition, EXEL-7647 inhibits cellular proliferation and EGFR pathway activation in the erlotinib-resistant H1975 cell line that harbors a double mutation (L858R and T790M) in the *EGFR* gene. *In vivo* efficacy studies show that EXEL-7647 substantially inhibited the growth of H1975 xenograft tumors and reduced both tumor EGFR signaling and tumor vessel density. Additionally, EXEL-7647, in contrast to erlotinib, substantially inhibited the growth and vascularization of MDA-MB-231 xenografts, a model which is more reliant on signaling through vascular endothelial growth factor receptors.

Conclusions: These studies provide a preclinical basis for clinical trials of XL647 in solid tumors and in patients bearing tumors that are resistant to existing EGFR-targeted therapies.

Receptor tyrosine kinases (RTK) are transmembrane proteins with an extracellular ligand binding domain and an intracellular tyrosine kinase catalytic domain. On binding to their cognate ligands, most RTKs dimerize and become activated through autophosphorylation of intracellular tyrosine residues. Activation of RTKs results in up-regulation of multiple cellular signaling pathways that promote cell growth, survival, and angiogenesis and normally occurs only in response to specific developmental or environmental stimuli. Inappropriate activation of RTKs via mutation, overexpression, or ectopic ligand production is a frequent feature of human tumor development and progression and is thought to be a major mechanism by which cancer cells subvert normal growth controls. Consequently, in recent years, modulation of RTK signal transduction has been an active area in oncology drug discovery (1, 2).

Authors' Affiliation: Exelixis, Inc., South San Francisco, California
Received 10/26/06; revised 1/17/07; accepted 2/27/07.
The costs of publication of this article were defrayed in part by the payment of page charges. This article must therefore be hereby marked *advertisement* in accordance with 18 U.S.C. Section 1734 solely to indicate this fact.
Requests for reprints: Alison H. Joly, New Lead Discovery, Exelixis, Inc., 210 East Grand Avenue, South San Francisco, CA 94083. Phone: 650-837-8217; Fax: 650-837-7580; E-mail: ajoly@exelixis.com.

doi:10.1158/1078-0432.CCR-06-2590

The epidermal growth factor receptor (EGFR; also known as ErbB1) and other ErbB family RTKs (ErbB2/HER-2/*neu*, ErbB3/HER-3, and ErbB4/HER-4) encoded by the c-erbB proto-oncogenes have been strongly implicated in cancer development and progression (reviewed in refs. 1, 3, 4). Overexpression of ErbB receptors and ligands has been documented in multiple tumor types, including lung, breast, colorectal, prostate, head and neck, and glioblastoma (3). Several mechanisms can cause aberrant receptor activation, resulting in tyrosine kinase activity, which is observed in cancer, including receptor overexpression, mutation, ligand-dependent receptor dimerization, and ligand-independent activation. For ErbB2, where a specific ligand has not been identified, activation occurs by homodimerization or heterodimerization alone, whereas ErbB3 does not have significant kinase activity (5). However, on activation, all four receptors are capable of signal transduction (6), causing activation of the ras/mitogen-activated protein kinase pathway, the phosphatidylinositol 3-kinase/AKT pathway, Src family kinases, and signal transducer and activator of transcription proteins. Activation of these pathways promotes cell proliferation, survival, and angiogenesis (reviewed in refs. 7, 8).

Activating somatic mutations in the *EGFR* gene are found in several human tumor types (9, 10). A deletion mutation in the extracellular domain of the receptor known as EGFR variant III (EGFRvIII) is overexpressed in breast, glioma, and lung cancers

(11) and exhibits ligand-independent, constitutive kinase activity (12). Small deletions or point mutations in the tyrosine kinase domain of EGFR are present in the tumors of non–small cell lung cancer (NSCLC) patients that experienced significant clinical responses following treatment with erlotinib or gefitinib (9, 10, 13). These mutations confer ligand independence or hypersensitivity to EGF and are more sensitive to inhibition by erlotinib or gefitinib than the wild-type (WT) receptor. However, some patients who initially experienced substantial objective tumor responses when treated with EGFR inhibitors have subsequently relapsed. In some cases, this resistance is associated with the acquisition of a "second site" point mutation (T790M) in the EGFR kinase domain (14). This residue is referred to as the "gatekeeper" threonine in EGFR and resides deep within the ATP-binding pocket. Analogous mutations in Bcr-Abl and c-Kit have been implicated in imatinib-resistant chronic myelogenous leukemia and gastrointestinal stromal tumors. *In vitro* experiments show that this gatekeeper mutation renders the activated EGFR insensitive to the inhibitory effects of erlotinib and gefitinib.

In addition to the ErbB family members that drive proliferation within the tumor, RTKs expressed in the supporting vasculature are important during tumor development. Vascular endothelial growth factors (VEGF) and their receptors (VEGFR1/Flt-1, VEGFR2/KDR, and VEGFR3/Flt-4) play critical roles in tumor angiogenesis and lymphangiogenesis (15). Like EGFR, activation of VEGF receptors (VEGFR) initiates the ras/mitogen-activated protein kinase cascade within endothelial cells that is responsible, in part, for the proangiogenic phenotype of VEGF (16). The Eph receptors comprise the largest subfamily of RTKs, members of which are also required for normal development of the vasculature and nervous system. Eph receptors and their cell-presented ligands, the ephrins, are frequently overexpressed in human tumors (17). In particular, ephrin type B subclass 4 receptor (EphB4) is up-regulated in prostate, breast, endometrial, small-cell lung, and gastrointestinal cancers (18–22). Overexpression of EphB4 in transgenic mice promotes tumor formation, whereas reduction of EphB4 in tumor cell lines inhibits growth both *in vitro* and *in vivo* (23).

Agents that selectively target EGFR, ErbB2, or VEGF have shown promising activity in clinical trials and several are now approved for use in select cancer indications. These include monoclonal antibodies targeting EGFR (cetuximab), ErbB2 (trastuzumab), VEGF (bevacizumab), and small-molecule EGFR inhibitors (erlotinib and gefitinib). Several lines of evidence suggest that simultaneous targeting of multiple members of the EGF and VEGF RTK families could provide improved and/or broader spectrum efficacy versus highly selective agents. For example, combinations of small-molecule EGFR and VEGFR inhibitors show improved efficacy in preclinical models compared with either agent alone (24). In addition, a small molecule that inhibits both EGFR and ErbB2 has shown activity in trastuzumab-resistant cells (25). We have identified a novel small-molecule inhibitor that targets multiple EGF and VEGF RTK family members, with the aim of affecting tumor cell growth and survival through direct effects on tumor cells and through inhibition of angiogenesis. This compound, EXEL-7647(XL647), is a potent inhibitor of EGFR, ErbB2, KDR, and EphB4 both enzymatically and in cellular assays of receptor phosphorylation. In addition to potent and long-lived inhibition of WT EGFR *in vivo*, EXEL-7647 retains significant EGFR inhibitory activity in the bronchoalveolar cell line, H1975, which harbors both an activating mutation, L858R, as well as the T790M mutation that confers resistance to erlotinib and gefitinib. When H1975 tumor xenografts were established in female severe combined immunodeficient mice, once-daily oral administration of EXEL-7647 significantly inhibited tumor growth in a dose-dependent manner. In contrast, erlotinib showed less efficacy and no dose dependence.

Immunohistochemical analysis of the tumors at the end of the dosing period showed a dose-dependent decrease in activated EGFR and its downstream effectors phosphorylated ERK ($pERK^{Thr202/Tyr204}$) and phosphorylated AKT ($pAKT^{Ser473}$), as well as decreases in tumor vasculature (CD31) and cell proliferation (Ki67), and an increase in apoptosis (terminal deoxynucleotidyl transferase–mediated dUTP nick end labeling).

EXEL-7647 also shows antiangiogenic activity *in vivo*, consistent with the potent inhibition of EXEL-7647 against the VEGFR family and EphB4 *in vitro*. When examined in MDA-MB-231 breast adenocarcinoma xenografts, which highly express VEGF (26, 27) and are not as reliant on EGFR signaling for tumor growth (28), EXEL-7647, but not erlotinib, showed potent and dose-dependent tumor growth inhibition and decreases in tumor vascularization (CD31). Taken together, these data show that EXEL-7647 is a potent inhibitor of RTKs that promote tumor epithelial cell growth and endothelial cell function that may have broad clinical utility particularly in tumors that are resistant to existing EGFR-targeted therapies.

Materials and Methods

Compounds

EXEL-7647 (29) was synthesized and purified in the Medicinal Chemistry Department at Exelixis, Inc. Gefitinib (30) and erlotinib (31) for use in biochemical and cellular assays were synthesized at Exelixis. For *in vitro* assays, a 10 mmol/L stock solution of each compound was prepared in DMSO and diluted in optimal assay buffers or culture medium. The final DMSO assay concentration did not exceed 0.3% (v/v). For *in vivo* studies, EXEL-7647 was formulated for oral administration by dissolution of the dry powder in sterile filtered (0.45 μm; Nalge Nunc International) saline (0.9% USP, Baxter Corp.) or in sterile water for injection (Baxter). For the A431 pharmacodynamic and efficacy studies, erlotinib and gefitinib were formulated as suspensions in 0.5% carboxymethylcellulose/5% ethanol. For the H1975 and MDA-MB-231 efficacy studies, erlotinib was formulated as a suspension of finely crushed clinical tablets (100 mg Tarceva tablets, Genentech, Inc.) suspended in water. All compounds were mixed by vortexing and sonicated in a water bath to disrupt large particles. All dosing solutions/suspensions were prepared fresh daily.

Kinase inhibition assays

Kinase activity and compound inhibition were investigated using one of three assay formats described below. The ATP concentration for each assay was equivalent to the K_m for each kinase. The kinase assay buffer contained 20 mmol/L Tris-HCl (pH 7.5), 10 mmol/L $MgCl_2$, 3 mmol/L $MnCl_2$, 1 mmol/L DTT, and 0.01% Triton X-100. Dose-response experiments were done using 10 different inhibitor concentrations in 384-well microtiter plates. IC_{50} values were calculated by nonlinear regression analysis using the four-variable equation: $Y = \text{min} + (\text{max} - \text{min}) / [1 + ([I] / IC_{50})^N]$, where Y is the observed signal, [I] is the inhibitor concentration, min is the background signal in the absence of enzyme (0% enzyme activity), max is the signal in the absence of inhibitor (100% enzyme activity), IC_{50} is the inhibitor concentration required at 50% enzyme inhibition, and N represents the empirical Hill slope as a measure of cooperativity.

^{33}P-Phosphoryl transfer kinase assay. Reactions were done in 384-well white, clear bottom, high-binding microtiter plates (Greiner). Plates were coated with 2 μg/well peptide substrate in a 50 μL volume. The coating buffer contained 40 μg/mL EphB4 substrate poly(Ala-Glu-Lys-Tyr) 6:2:5:1 (Perkin-Elmer), 22.5 mmol/L Na_2CO_3, 27.5 mmol/L $NaHCO_3$, 150 mmol/L NaCl, and 3 mmol/L NaN_3. The coated plates were washed once with 50 μL assay buffer following overnight incubation at room temperature. Test compound and either 5 nmol/L EphB4 (residues E605-E890 of human EphB4 containing a six histidine NH_2-terminal tag, which was expressed in a baculovirus expression system and purified using metal chelate chromatography), 4 nmol/L insulin-like growth factor-I receptor (residues M954-C1367 of human insulin-like growth factor-I receptor, Proqinase GmbH), or 15 nmol/L insulin receptor 1 (residues P948-S1343 of human insulin receptor 1, Proqinase) were combined with [^{33}P]γ-ATP (5 μmol/L, 3.3 μCi/nmol) in a total volume of 20 μL. The reaction mixture was incubated at room temperature for 1.5 to 2.5 h and terminated by aspiration. The microtiter plates were subsequently washed six times with 0.05% Tween-PBS buffer. Scintillation fluid (50 μL/well) was added and incorporated ^{33}P was measured by liquid scintillation spectrometry using a MicroBeta scintillation counter (Perkin-Elmer).

Luciferase-coupled chemiluminescence assay. Kinase activity was measured as the percentage of ATP consumed following the kinase reaction using luciferase-luciferin–coupled chemiluminescence. Reactions were conducted in 384-well white, medium-binding microtiter plates (Greiner). Kinase reactions were initiated by combining test compound, 3 μmol/L ATP, 1.6 μmol/L substrate [poly(Glu,Tyr) 4:1; Perkin-Elmer], and either EGFR (7 nmol/L, residues H672-A1210 of human EGFR, Proqinase) or KDR (5 nmol/L, residues D807-V1356 of human KDR, Proqinase) in a 20 μL volume. The reaction mixture was incubated at room temperature for 4 h. Following the kinase reaction, a 20 μL aliquot of Kinase Glo (Promega) was added and luminescence signal was measured using a Victor2 plate reader (Perkin-Elmer). Total ATP consumption was limited to 50%.

AlphaScreen tyrosine kinase assay. Donor beads coated with streptavidin and acceptor beads coated with PY100 anti-phosphotyrosine antibody (Perkin-Elmer) were used. Biotinylated poly(Glu,Tyr) 4:1 was used as the substrate. Substrate phosphorylation was measured by luminescence following donor-acceptor bead addition followed by complex formation. Test compound, 3 μmol/L ATP, 3 nmol/L biotinylated poly(Glu,Tyr) 4:1, and 1 nmol/L ErbB2 (residues Q679-V1255 of human ErbB2, Proqinase) or Flt-4 (residues D725-R1298 of human Flt-4, Proqinase) were combined in a volume of 20 μL in a 384-well white, medium-binding microtiter plate (Greiner). Reaction mixtures were incubated for 1 h at room temperature. Reactions were quenched by addition of 10 μL of 15 to 30 μg/mL AlphaScreen bead suspension containing 75 mmol/L HEPES (pH 7.4), 300 mmol/L NaCl, 120 mmol/L EDTA, 0.3% bovine serum albumin, and 0.03% Tween 20. After 2 to 16 h of incubation at room temperature, plates were read using an AlphaQuest reader (Perkin-Elmer).

Cell lines and cell culture conditions

The A431 human epidermoid carcinoma cell line was purchased from the American Type Culture Collection, and MDA-MB-231 human adenocarcinoma cells were generously provided by Georgetown University. Both cell lines were maintained and propagated as monolayer cultures in DMEM (Mediatech) containing L-glutamine supplemented with 10% heat-inactivated fetal bovine serum (Hyclone), 100 units/mL penicillin G, 100 μg/mL streptomycin (1% penicillin/streptomycin, Mediatech), and 1% nonessential amino acids (Mediatech) at 37°C in a humidified 5% CO_2 incubator. The NSCLC adenocarcinoma H1975 (American Type Culture Collection) and the Lx-1 squamous cell carcinoma (Department of Oncology Drug Discovery, Bristol-Myers Squibb) cell lines were maintained in complete RPMI 1640 (30-2,001; American Type Culture Collection; containing L-glutamine supplemented with 10% heat-inactivated fetal bovine serum, 1% penicillin/streptomycin, and 1% nonessential amino acids) at 37°C in a humidified 5% CO_2 incubator.

Cellular assays

WT EGFR autophosphorylation. A431 cells were seeded at 5×10^4 per well in 96-well microtiter plates (3904 Costar, VWR) and incubated in fully supplemented DMEM for 16 h after which growth medium was replaced with serum-free DMEM and the cells were incubated for an additional 24 h. Serial dilutions of EXEL-7647 (in triplicate) in serum-free medium were added to the quiescent cells and incubated for 1 h before stimulation with 100 ng/mL recombinant human EGF (R&D Systems) for 10 min. Negative control wells did not receive EGF. After treatment, cell monolayers were washed with cold PBS and immediately lysed with cold lysis buffer [50 mmol/L Tris-HCl (pH 8.0), 150 mmol/L NaCl, 10% glycerol, 1% NP40, 0.1% SDS, 0.5% sodium deoxycholate, 1 mmol/L EDTA, 50 mmol/L NaF, 1 mmol/L sodium pyrophosphate, 1 mmol/L sodium orthovanadate, 2 mmol/L phenylmethylsulfonyl fluoride, 10 μg/mL aprotinin, 5 μg/mL leupeptin, 5 μg/mL pepstatin]. Lysates were centrifuged, transferred to 96-well streptavidin-coated plates (Pierce) containing biotin-conjugated, mouse monoclonal anti-human EGFR (2 μg/mL; Research Diagnostics), and incubated for 2 h. Plates were washed thrice with TBST [25 mmol/L Tris, 150 mmol/L NaCl (pH 7.2), 0.1% bovine serum albumin, and 0.05% Tween 20] and incubated with horseradish peroxidase–conjugated anti-phosphotyrosine antibody (1:10,000; Zymed Laboratories). Horseradish peroxidase activity was determined by reading the plates in a Victor2 plate reader following addition of the ELISA Femto substrate (Pierce). IC_{50} values were determined based on total EGFR tyrosine phosphorylation with EXEL-7647 treatment versus total EGFR tyrosine phosphorylation with growth factor treatment alone, normalized to receptor levels.

Phosphorylation and proliferation assays using EGFR mutants

Expression vector cloning. A clone corresponding to the longest EGFR isoform (Genbank accession no. NM_005228.3/NP_005219.2 #21-176, Upstate Biotechnology) was used as a template to produce two mutant EGFR genes (coding for L858R and L861Q) by site-directed mutagenesis. The WT and the two sequence-verified mutants were transferred to a COOH-terminal Flag-tagged retroviral cytomegalovirus promoter-driven mammalian expression vector. The two Tet-On expression vectors, EGFR WT (Tet-On) and EGFRvIII (Tet-On), which were COOH-terminally Flag tagged, were generously provided by Dr. Abhijit Guha (University of Toronto, Toronto, Ontario, Canada).

Transient transfections. Transient transfections of Lx-1 cells were done using LipofectAMINE 2000 (Invitrogen) according to the manufacturer's protocol. For transfections of the WT, L858R, and L861Q constructs, 1 μg plasmid DNA was used for each transfection (each well of a 12-well plate). For transfections of Tet-controlled EGFR WT and variant III constructs, 0.5 μg of either construct was combined with 0.5 μg of the pTet-On plasmid (BD Biosciences) for each transfection. Cells were harvested 24 h after transfection and replated in either 96-well plates (4×10^4 cells per well) for compound treatments or 12-well plates (2×10^5 cells) for immunoblot assays. Expression of the EGFRvIII transgene was induced 24 h after transfection by adding 1 μg/mL doxycycline to the medium. These cells were maintained in the presence of doxycycline for the remainder of the experiment. After a 12-h incubation, the cells were serum starved (in fetal bovine serum–free medium) and immediately treated with the indicated compounds in triplicate for 24 h followed by a 10-min treatment with recombinant human EGF (100 ng/mL). Whole-cell lysates were made by adding 125 μL radioimmunoprecipitation assay buffer (Boston Bioproducts) containing protease inhibitors (Protease Inhibitor Cocktail Tablets, Roche) in addition to 50 mmol/L NaF, 1 mmol/L sodium pyrophosphate, 1 mmol/L sodium orthovanadate, 2 mmol/L phenylmethylsulfonyl fluoride, 10 μg/mL aprotinin, and 5 μg/mL leupeptin in each well for either EGFR phosphorylation ELISA or immunoblot.

EGFR ELISA. Reacti-Bind streptavidin-coated plates (Pierce) were coated with 2 μg/mL biotin-conjugated anti-Flag antibody (Sigma). Whole-cell lysates (10 μg) were then added to the anti-Flag–coated wells in a final volume of 100 μL for 2 h at room temperature and then washed thrice with TBST. The anti-phosphotyrosine horseradish peroxidase–coupled secondary antibody (1:10,000; Zymed) was used to detect phosphorylated EGFR (pEGFR; 1 h at room temperature followed by three washes with TBST). Horseradish peroxidase activity was determined by reading the plates in a Victor2 plate reader following addition of the ELISA Femto substrate.

Cell viability assay. Growth inhibition of H1975 and A431 cells by increasing concentrations of EXEL-7647, gefitinib, or erlotinib was determined by seeding 5×10^3 cells per well in 96-well plates. The following day, cells were washed once with low-serum RPMI 1640 (0.1% fetal bovine serum, 1% nonessential amino acids, and 1% penicillin/streptomycin), after which 90 μL of the low-serum RPMI 1640 were added. Test compounds were diluted to 10 times the test concentrations and 10 μL were added to triplicate wells for a 72-h incubation. Cell viability was determined using Alamar blue solution (Biosource).

Analysis of H1975 cell lysates. For the H1975 immunoblot studies, 3×10^5 cells were plated in each well (12-well plate) and incubated for 16 h in complete RPMI 1640, rinsed with fetal bovine serum–free RPMI 1640, and incubated with serial dilutions of test compounds in fetal bovine serum–free medium for 2 h followed by stimulation with 100 ng/mL human recombinant EGF for 10 min. Whole-cell protein lysates were prepared as described above and centrifuged for 10 min at 13,000 × *g* at 4°C to remove any insoluble material. Total protein was determined using bicinchoninic acid reagent and an equal amount of protein was combined with LDS loading buffer (Invitrogen) according to the manufacturer's instructions. Proteins were separated by gel electrophoresis on 4% to 15% polyacrylamide gels, transferred to nitrocellulose membranes, and detected by immunoblotting. Antibody-antigen complexes were detected using chemiluminescence. The following antibodies from Cell Signaling Technology were used at a 1:1,000 dilution: anti-EGFR, anti-pEGFR^{Tyr1068}, anti-AKT, anti-pAKT^{Ser473}, anti-ERK, and anti-pERK$^{Thr202/Tyr204}$. The anti-β-actin primary antibody (Accurate Chemical and Scientific) was used at 1:10,000 and the horseradish peroxidase–coupled secondary antibodies were purchased from Jackson ImmunoResearch and used at 1:5,000.

In vivo studies

Female severe combined immunodeficient mice and female athymic nude mice (NCr), 5 to 8 weeks of age and weighing ~20 to 25 g, were purchased from The Jackson Laboratory and Taconic, respectively. The animals were housed at the Exelixis vivarium facilities according to guidelines outlined by the Exelixis Institutional Animal Care and Use Committee. During all studies, animals were provided food and water *ad libitum* and housed in a room conditioned at 70°F to 75°F and 60% relative humidity.

H1975, A431, or MDA-MB-231 cells were harvested from exponentially growing cultures, detached by brief trypsinization, washed twice in cold HBSS, resuspended in ice-cold HBSS, and implanted either s.c. (H1975, 3×10^6 cells per mouse) or i.d. (A431, 1×10^6 cells per mouse) into the dorsal hind flank or s.c. into the mammary fat pad (MDA-MB-231, 1×10^6 cells per mouse). Palpable tumors were measured by caliper twice weekly until the mean tumor weight was in the range of ~80 to 120 mg. Tumor weight was determined by measuring perpendicular diameters with a caliper and multiplying the measurements of diameters in two dimensions: tumor volume (mm^3) / 2 = length (mm) × width^2 (mm^2) / 2. Tumor weight (mg) was extrapolated from tumor volume (mm^3) by assuming a conversion factor of 1. On the appropriate day after implantation, mice were grouped (10 mice per group) such that the group mean tumor weight was ~100 ± 15 mg. The mean tumor weight of each animal in the respective control and treatment groups was determined twice weekly during the dosing periods. The response of tumors to treatment was determined by comparing the mean tumor weight of the treatment group with the appropriate control group. Percentage inhibition of tumor growth was determined with the following formula: Percentage inhibition = $100 \times [1 - (X_f - X_o) / (Y_f - Y_o)]$, where X_f and Y_f are the mean tumor weights of the treatment and control groups, respectively, on day f, and X_o and Y_o are the mean tumor weights of treatment and control groups respectively, on day zero (staged tumor weights after grouping).

In vivo target modulation

EGFR autophosphorylation was evaluated in tumor xenografts derived from A431 cells that overexpress WT EGFRs (29). Tumor-bearing mice were given either EXEL-7647, erlotinib, or gefitinib at 100 mg/kg and tumors were harvested 1 to 72 h later. Half an hour before respective time point, EGF (50 μg/mouse; R&D Systems) was given via i.v. bolus injection with tumors dissected 30 min later and tumor extracts were prepared by homogenization (Polytron PT 10/35, Brinkmann) in 10 volumes of ice-cold lysis buffer [50 mmol/L Tris-HCl (pH 8.0), 150 mmol/L NaCl, 1% NP40, 0.1% SDS, 0.5% deoxycholate, 1 mmol/L EDTA, 50 mmol/L NaF, 1 mmol/L sodium pyrophosphate, 1 mmol/L orthovanadate, 2 mmol/L phenylmethylsulfonyl fluoride, 10 μg/mL aprotinin, 5 μg/mL leupeptin, 5 μg/mL pepstatin A]. Lysates were clarified by centrifugation (20,000 × *g* for 10 min at 4°C) and EGFR tyrosine phosphorylation levels were determined by ELISA (as described above).

Determination of plasma levels of EXEL-7647, gefitinib, or erlotinib

For determination of compound levels in plasma following oral administration of EXEL-7647, gefitinib, or erlotinib, whole blood was placed in heparinized Eppendorf tubes on ice and centrifuged at 20,000 × *g* for 4 min. The plasma supernatant (50 μL) was added to 100 μL internal standard solution (250 ng/mL internal standard in acetonitrile), mixed by vortexing, and centrifuged. Sample extract (20 μL) was assayed for EXEL-7647, gefitinib, or erlotinib by LC/MS/MS analysis. Plasma levels were calculated using an authentic standard curve for each compound. The limit of quantification was 0.004 μmol/L (2 ng/mL) for EXEL-7647, gefitinib, and erlotinib. Mean values and SD were calculated for each time point and dose concentration was assessed.

Immunohistochemistry

For immunohistochemical analysis of H1975 and MDA-MB-231 xenografts, tumors were excised after euthanasia and fixed in zinc fixative (BD Biosciences) for 48 h before being processed into paraffin blocks. Serial sections at 5 μm were obtained from the area of largest possible surface for each tumor and stained using standard methods. The following antibodies were used: Ki67 (SP6; Labvision), CD31 (MECA.32; BD Biosciences), pERK$^{Thr202/Tyr204}$ (phospho-p44/42 mitogen-activated protein kinase; Cell Signaling Technology), pAKT^{Ser473} (Cell Signaling Technology), and pEGFR^{Tyr1068} (Cell Signaling Technology). For immunofluorescent staining, sections were then incubated with Alexa 594–conjugted goat anti-rabbit secondary antibody (Invitrogen) and mounted in Fluorescent Mounting Medium (DAKO) containing 4′,6-diamidino-2-phenylindole (Molecular Probes) as a nuclear counterstain. Fluorescent staining was visualized using a Zeiss AxioImager and digitally captured using a Zeiss high-resolution camera coupled to AxioVision image analysis software. Two to three nonoverlapping representative fields were captured at ×200 or ×400 magnification depending on histologic readout and quantified using the integrated morphometric analysis functions in Metamorph software (Universal Imaging Corp.). Apoptotic cells were detected using terminal deoxynucleotidyl transferase–mediated dUTP nick end labeling *in situ* cell death detection kit according to the manufacturer's instructions (Roche Diagnostics GmbH).

CD31-positive tumor vessels, Ki67-positive proliferating cells, and pERK staining in each tumor section were identified and quantified

using the integrated morphometric analysis functions in the ACIS automatic cellular imaging system (Clarient, Inc.) and reviewed by a blinded observer. Number of CD31-positive vessels were identified across 5 to 10 randomly chosen fields of equal size at ×100 magnification in viable tumor tissue and calculated as number of vessels per square millimeter for each tumor, averaged for each treatment group, and compared with vehicle-treated controls. Percentage Ki67-positive cells were calculated as the ratio between Ki67-positive cells divided by the total number of cells identified across 5 to 10 randomly chosen fields of equal size in viable tumor tissue. The results for each tumor and treatment group were averaged and compared with vehicle-treated controls. The level of pERK staining was determined as described above and calculated as the ratio of antibody staining divided by the total number of cells identified, averaged for each treatment group, and compared with vehicle-treated controls.

Statistics

Results are presented as mean ± SD or SE as indicated for each graph or table. For IC_{50} comparison in the A431 cell viability experiment, two sample Student's *t* tests were applied to determine *P* values for each IC_{50} pair assuming that the random fluctuations of replicates around the dose-response curve are distributed [log]normally with the individual replicates used as the 'sample size' for the *t* test (nine point dose response done in triplicate). For statistical analysis of immunohistochemical results from *in vivo* studies, two-tailed Student's *t* test analysis and Bonferroni correction were done to identify significant differences compared with vehicle control group (multiple use of a single vehicle control group) with a cumulative minimal requirement of $P < 0.05$. Final tumor weight measurements at the end of the H1975 efficacy study and percentage pEGFR, pAKT, Ki67 index, CD31, and terminal deoxynucleotidyl transferase–mediated dUTP nick end labeling in H1975 xenografts were analyzed with one-way ANOVA followed by post hoc Student-Newman-Keul analysis for determination of statistical differences between EXEL-7647 and erlotinib.

Results

In vitro *target inhibition profile of EXEL-7647.* EXEL-7647 was optimized as an inhibitor of a spectrum of growth-promoting and angiogenic RTKs to simultaneously block tumor growth and vascularization. In particular, EXEL-7647 potently inhibits the EGF/ErbB2, VEGF, and ephrin RTK families (Table 1). Mechanism of action studies for EGFR, ErbB2, KDR, and EphB4 confirmed that EXEL-7647 is a reversible and ATP competitive inhibitor (data not shown). EXEL-7647 was inactive against a panel of 10 tyrosine kinases (including the insulin and the insulin-like growth factor-1 receptor) and 55 serine-threonine kinases (including cyclin-dependent kinases, stress-activated protein kinases, and protein kinase C isoforms).

Table 1. *In vitro* kinase inhibition profile of EXEL-7647

Kinase	IC_{50} ± SD (nmol/L)
EGFR	0.3 ± 0.1
ErbB2	16 ± 3
KDR	1.5 ± 0.2
Flt-4	8.7 ± 0.6
EphB4	1.4 ± 0.2
IGF1R	>10,000
InsR	>26,000

NOTE: Results are mean ± SD of at least three independent determinations.
Abbreviations: IGF1R, insulin-like growth factor-I receptor; InsR, insulin receptor.

Potent biochemical inhibition of WT EGFR was confirmed in a cell-based assay using the A431 cell line that endogenously expresses elevated levels of EGFR (31). As shown in Table 2, EXEL-7647 shows potent inhibition of EGFR with a IC_{50} value of 1 nmol/L. Activating somatic mutations resulting in either deletions or amino acid substitutions in the kinase domain of the *EGFR* gene have been found to correlate with clinical response to the EGFR RTK inhibitors, gefitinib and erlotinib, in NSCLC patients (9, 10). To assess the activity of EXEL-7647 against these EGFR mutants, WT, L861Q, and L858R mutant EGFRs were overexpressed by transient transfection in the squamous cell carcinoma cell line, Lx-1, and EGFR activation was measured. Lx-1 cells were chosen for these studies because EGFR expression is undetectable in this cell line. In this assay system, EXEL-7647 inhibited the WT EGFR with a IC_{50} value of 12 nmol/L. Consistent with previous reports (9, 10), the mutant EGFRs seem to be more sensitive to EGFR inhibition than the WT receptor (Table 2). EGFRvIII is frequently present and amplified in malignant gliomas and exhibits ligand-independent kinase activity (11, 12). EXEL-7647 was assessed for inhibition of the activity of EGFRvIII in EGFR phosphorylation assays. A tetracycline-inducible (Tet-On) system was used to express both the WT and the EGFRvIII construct in Lx-1 cells. In this assay system, EXEL-7647 inhibited the WT and mutant EGFRvIII with IC_{50} values of 5 and 74 nmol/L, respectively (Table 2).

EXEL-7647 inhibits mutant EGFR resistant to gefitinib and erlotinib. An EGFR mutation (T790M) has been identified in NSCLC patients who have activating mutations in the *EGFR* gene, who initially responded to gefitinib or erlotinib but later developed drug resistance (14). To assess the ability of EXEL-7647 and other EGFR inhibitors to inhibit the activity of an EGFR harboring the T790M mutation, cell viability assays were done using the NSCLC cell line H1975 that contains both an activating (L858R) and resistance-associated mutation (T790M). For comparison, cell viability assays were done in parallel using A431 cells, which express WT EGFR (29). In A431 cells, EXEL-7647, gefitinib, and erlotinib reduced cell viability with IC_{50} values of 13, 31, and 84 nmol/L, with 95% confidence intervals of 10 to 15, 23 to 39, and 67 to 100 nmol/L, respectively (Fig. 1A). As expected, H1975 cells are more resistant to EGFR inhibitors than cells harboring the WT receptor. However, H1975 cells are 11 and 17 times more sensitive to EXEL-7647 (IC_{50}, 0.92 μmol/L) than to gefitinib (IC_{50}, 10.41 μmol/L) and erlotinib (IC_{50}, 16.14 μmol/L), with 95% confidence intervals of 0.84 to 1.01, 8.80 to 12.02, and 9.34 to 22.94 μmol/L, respectively (Fig. 1A). Student's *t* test analysis confirmed that EXEL-7647 is significantly more potent in the H1975 cell viability assay than either gefitinib or erlotinib ($P < 0.001$). Analysis of EGFR-mediated signaling in H1975 cells following treatment with the different inhibitors supports the observations made using the viability assay. As expected, EGFR in H1975 cells is constitutively phosphorylated (Fig. 1B). Downstream signaling pathways are also activated as judged by the constitutive phosphorylation of both AKT and ERK. Addition of exogenous EGF further increases EGFR, AKT, and ERK phosphorylation. Treatment with gefitinib or erlotinib has minimal effect on the phosphorylation of EGFR, AKT, or ERK

Table 2. Inhibition of WT and mutant EGFR phosphorylation by EXEL-7647 in cells

EGFR	IC_{50} (nmol/L)
WT (A431)	1
WT (pCMV/Lx-1)	12
L858R (pCMV/Lx-1)	5
L861Q (pCMV/Lx-1)	10
WT (pTet-On/Lx-1)	5
Variant III (pTet-On/Lx-1)	74

when tested at concentrations up to 30 μmol/L. In contrast, treatment with 10 μmol/L EXEL-7647 results in an almost complete inhibition of EGFR, AKT, and ERK phosphorylation (Fig. 1B). These results are consistent with the effects observed in the viability assay and show that EXEL-7647 retains significant potency against the T790M EGFR mutant.

EXEL-7647 inhibits the WT and the gatekeeper mutant EGFR in vivo. Consistent with *in vitro* data, EXEL-7647 shows long-lasting inhibition of WT EGFR autophosphorylation in the A431 xenograft model, which overexpresses WT EGFR (32). Single oral doses of 100 mg/kg EXEL-7647 were given to A431 tumor-bearing athymic nude mice and tumors were harvested at various times between 1 and 72 h later, with administration of EGF 0.5 h before each tumor harvest. EGFR phosphorylation was substantially inhibited (>90%) throughout the entire time course of this study (Fig. 2A). At the 72-h time point, phosphorylation of EGFR in response to EGF is still maximally decreased, despite the plasma concentration of EXEL-7647 being <1 μmol/L. A second time course study was conducted with gefitinib and erlotinib, to compare the duration of action of EXEL-7647 with clinically validated EGFR inhibitors. Gefitinib and erlotinib showed substantial inhibition of EGFR phosphorylation in this model at the 4- and 8-h time points, but little or no inhibition was evident at subsequent time points (Fig. 2A).

Consistent with the pharmacodynamic assays described above, EXEL-7647 shows potent and dose-dependent tumor growth inhibition in the A431 xenograft model. Substantial tumor growth inhibition of 77% was achieved by once-daily oral administration of 10 mg/kg EXEL-7647, whereas the highest dose of 100 mg/kg causes tumor regression to 65% below the starting tumor size (Fig. 2B). This result is consistent with the potent antiproliferative activity of EXEL-7647 in A431 cells (Fig. 1A).

In cellular assays of EGFR activation, EXEL-7647 has reduced potency against the T790M EGFR mutant compared with WT EGFR; however, the concentrations required to inhibit mutant EGFR in H1975 cells are in the same range as the plasma levels of EXEL-7647 achieved following oral dosing (Fig. 2A). To examine the *in vivo* effects of EXEL-7647 on the T790M mutant EGFR, H1975 human tumor xenografts were established s.c. in female severe combined immunodeficient mice and allowed to reach ~100 mg before once-daily oral administration of EXEL-7647 at 10, 30, and 100 mg/kg or erlotinib at 30 and 100 mg/kg for 14 days. Figure 3 shows that EXEL-7647 substantially inhibited tumor growth in a dose-dependent manner when compared with the vehicle-treated control group. Tumor growth inhibition reached 33%, 66%, and 92% for the

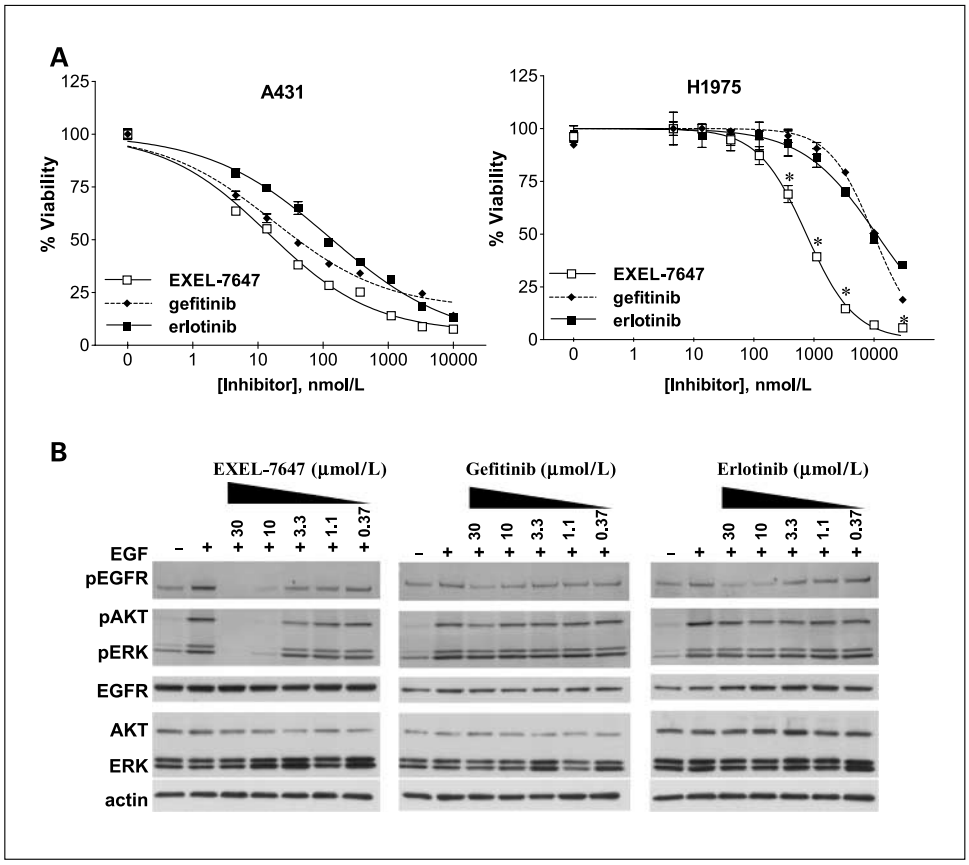

Fig. 1. Differential inhibition of cell viability and EGFR pathway activity following EGFR inhibitor treatment in H1975 and A431 cells. *A,* dose-response curves comparing the effect of EGFR inhibitors, EXEL-7647, gefitinib, and erlotinib on the viability of the bronchoalveolar cell line H1975 that harbors both an activating mutation in EGFR (L858R) in addition to the resistance-associated mutation (T790M) and A431 cells that contain WT EGFR. Cell viability was determined 3 d after the administration of compounds. This experiment was done in duplicate and the average is reported in Results. *, $P < 0.001$, significant difference between IC_{50} values of EXEL-7647 and gefitinib and erlotinib, Student's *t* test. *B,* immunoblot analysis of whole-cell lysates from H1975 treated with the indicated EGFR inhibitors (see Materials and Methods).

10, 30, and 100 mg/kg dose groups ($P < 0.005$ when compared with the vehicle-treated control group), respectively, with a calculated ED_{50} of 17 mg/kg. Consistent with these data, the plasma concentrations of EXEL-7647 following the final dose increased in a dose-dependent manner (C_{max} was 1, 3, and 15 μmol/L for the 10, 30, and 100 mg/kg dose groups, respectively; T_{max} was 4 h). These end of study plasma levels determined after 14 consecutive days of dosing indicate a 1.5-fold accumulation of EXEL-7647 in the plasma on repeat dosing when compared with a single dose (i.e., at 4 h after a single dose of 100 mg/kg, the plasma concentration was 10.6 μmol/L, whereas at 4 h following the 14th daily dose, the plasma level was 15 μmol/L). EXEL-7647 was well tolerated at all dosing levels throughout the course of the experiment as evidenced by the lack of body weight loss in all groups (Fig. 3, *inset*). In contrast to EXEL-7647, erlotinib only modestly inhibited H1975 xenograft tumor growth in this study (Fig. 3). Tumor growth inhibition was statistically significant ($P < 0.005$) when compared with the vehicle-treated control group, but modest and not dose independent (33-37% inhibition for the 30 and 100 mg/kg dose groups). For erlotinib, efficacy was likely limited for mechanistic, rather than pharmacokinetic, reasons because last dose pharmacokinetic profiling showed that the erlotinib plasma exposure was substantial and increased with dose (C_{max} was 12 and 27 μmol/L, respectively, for the 30 and 100 mg/kg dose groups; T_{max} was 4 h). Statistical analysis by one-way ANOVA with post hoc Student-Newman-Keul revealed that EXEL-7647 was significantly more potent in preventing tumor growth in this xenograft model than erlotinib ($P = 0.01$, dose to dose comparison).

Immunohistochemical analyses of the tumors at the end of the dosing period showed that, in contrast to erlotinib, EXEL-7647 treatment was associated with a significant ($P < 0.001$) and dose-dependent reduction in the levels of pEGFR when compared with vehicle-treated tumors (Fig. 4; Table 3). In addition, EXEL-7647 showed significant and dose-dependent decreases in phosphorylation of the EGFR effectors AKT and ERK (Table 3), whereas erlotinib showed moderate decreases (Table 3). Further immunohistochemical analyses showed that EXEL-7647 increased the percentage of terminal deoxynucleotidyl transferase–mediated dUTP nick end labeling–positive cells with a 7- to 16-fold increase in apoptosis compared with vehicle-treated tumors (Table 4). The percentage of CD31-positive vessels in viable tumor tissue was also significantly ($P < 0.005$) decreased following EXEL-7647 treatment, indicating a dose-dependent loss of microvessel density (Fig. 4; Table 4). Similar decreases in the percentage of Ki67-expressing cells (Ki67 index) in the H1975 tumors were also observed at all dose levels, indicating a significant reduction in proliferating cells in the tumors at the end of the study. Tumors from the groups that received erlotinib at 30 and 100 mg/kg showed moderate effects on apoptosis and Ki67 index and no reduction in number of tumor vessels. Thus, treatment of H1975 xenografts with EXEL-7647 results in significant inhibition of EGFR and its downstream effectors *in vivo*, resulting in inhibition of tumor cell proliferation and vascularization and an induction of tumor cell apoptosis. The observed decreases in pEGFR and pAKT in the EXEL-7647–treated groups as well as the effects on tumor cell proliferation, vascularization, and apoptosis were significantly more potent than those observed

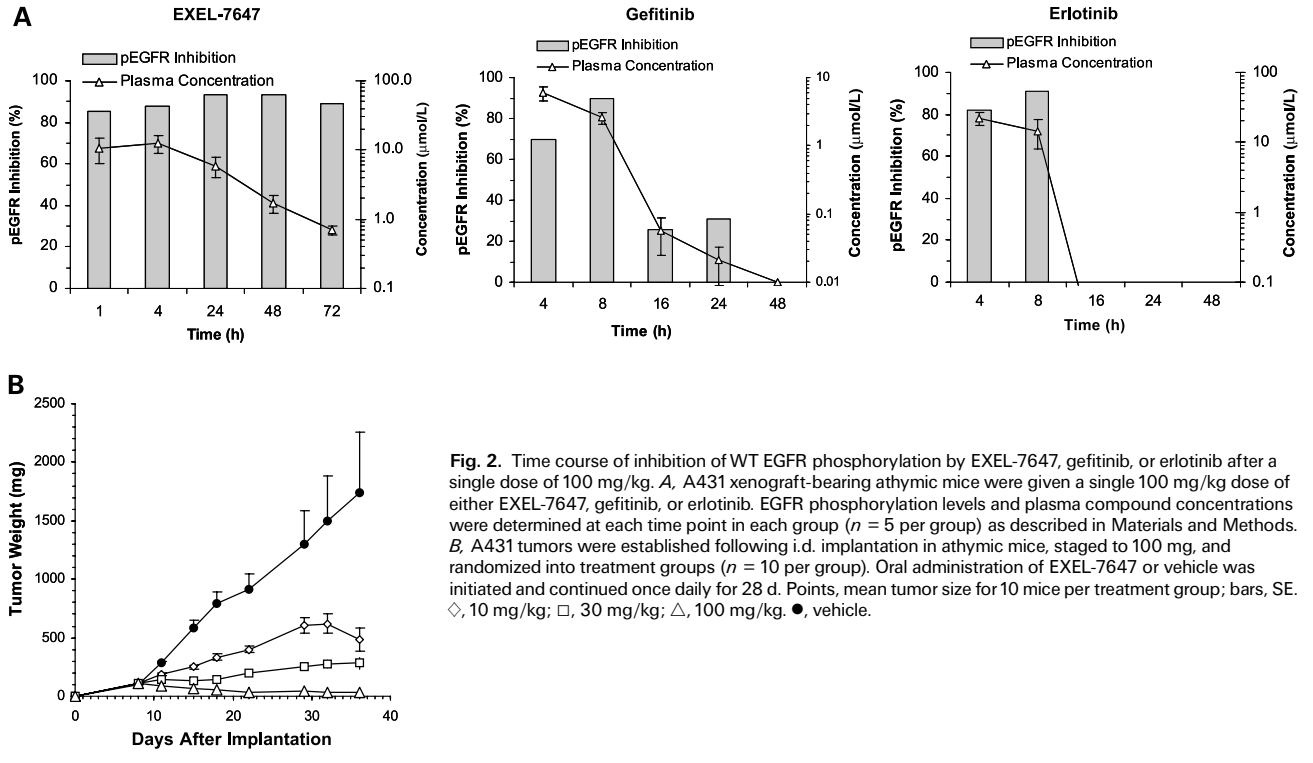

Fig. 2. Time course of inhibition of WT EGFR phosphorylation by EXEL-7647, gefitinib, or erlotinib after a single dose of 100 mg/kg. *A,* A431 xenograft-bearing athymic mice were given a single 100 mg/kg dose of either EXEL-7647, gefitinib, or erlotinib. EGFR phosphorylation levels and plasma compound concentrations were determined at each time point in each group ($n = 5$ per group) as described in Materials and Methods. *B,* A431 tumors were established following i.d. implantation in athymic mice, staged to 100 mg, and randomized into treatment groups ($n = 10$ per group). Oral administration of EXEL-7647 or vehicle was initiated and continued once daily for 28 d. Points, mean tumor size for 10 mice per treatment group; bars, SE. ◇, 10 mg/kg; □, 30 mg/kg; △, 100 mg/kg. ●, vehicle.

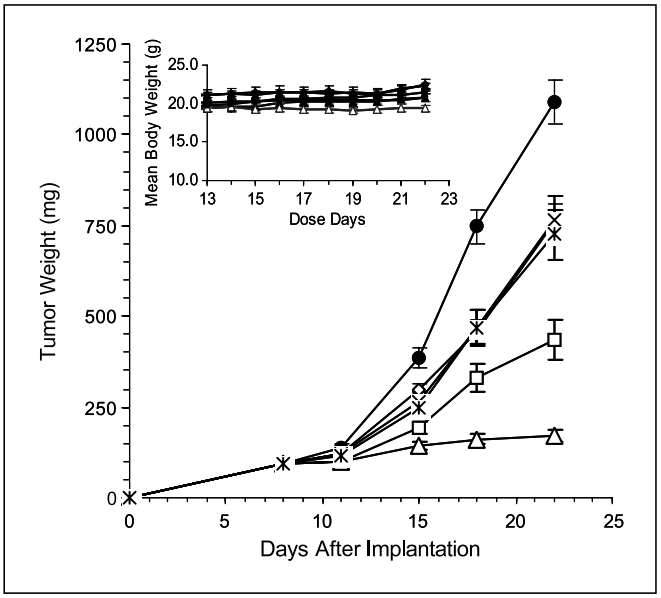

Fig. 3. Tumor growth inhibition of EXEL-7647 or erlotinib in H1975 xenografts. Tumors were established following s.c. implantation in severe combined immunodeficient mice, staged to 100 mg, and randomized into treatment groups (n = 10 per group). Oral administration of EXEL-7647, erlotinib, or vehicle was initiated and continued once daily for 14 d. Points, mean tumor size for 10 mice per treatment group; bars, SE. EXEL-7647 (◇, 10 mg/kg/d; □, 30 mg/kg/d; △, 100 mg/kg/d), vehicle (●), or erlotinib at either 100 mg/kg/d (X) or 30 mg/kg (*).

in the erlotinib-treated groups ($P < 0.01$; one site ANOVA with post hoc Student-Newman-Keul analysis).

The A431 and H1975 xenograft studies described here examined the *in vivo* effects of EXEL-7647 on WT and mutant EGFR; however, as mentioned previously (Table 1), EXEL-7647 is a RTK inhibitor that inhibits a spectrum of growth-promoting and proangiogenic RTKs, including VEGFRs. Therefore, to examine the effects of EXEL-7647 and erlotinib in a xenograft model that is less dependent on EGFR signaling for tumor growth (28) and expressing high levels of VEGF (26, 27), MDA-MB-231 human breast adenocarcinoma xenograft tumors were established in the mammary fat pad of athymic nude mice. When tumors reached an approximate weight of 100 mg, once-daily oral administration of EXEL-7647 or erlotinib at 30 or 100 mg/kg was initiated and continued for 14 days. Figure 5A shows that EXEL-7647 at 30 and 100 mg/kg significantly inhibited tumor growth by 35% and 81%, respectively, when compared with the vehicle-treated control group ($P < 0.005$). In contrast, erlotinib did not significantly inhibit tumor growth in this model (Fig. 5B) exhibiting tumor growth inhibition of 19% and 17% in the 30 and 100 mg/kg groups, respectively, which did not reach statistical significance. Immunohistochemical analysis of the tumors at the end of the study (Table 5) showed that, consistent with the inhibitory activity against VEGFRs, there was a significant decrease in tumor vessel density (CD31) in the EXEL-7647 – treated groups but not in the erlotinib-treated groups compared with respective vehicle control groups. In addition, EXEL-7647 treatment resulted in a significant decrease in cell proliferation (Ki67; Table 5). These data indicate that EXEL-7647 significantly inhibited tumor growth in a xenograft model that does not exhibit a strong dependency on EGFR signaling and supports the hypothesis that simultaneous targeting of a spectrum of growth-promoting and proangiogenic RTKs translates into broader efficacy than agents that exhibit a more selective RTK inhibition profile.

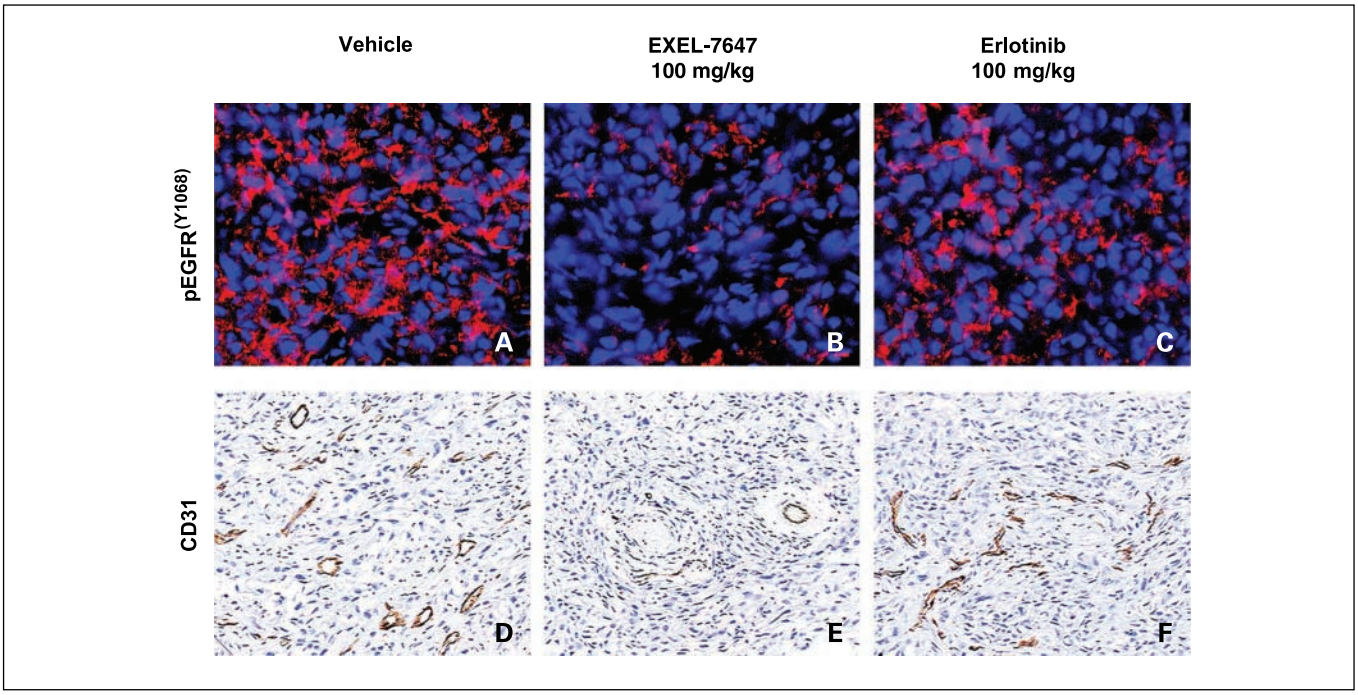

Fig. 4. Immunohistochemical analysis of pEGFR- and CD31-positive tumor vessels in H1975 xenografts. Daily administration of EXEL-7647 at 100 mg/kg to mice bearing H1975 xenografts results in significant decrease in pEGFR staining and number of CD31-positive tumor vessels compared with vehicle control. Tumors were harvested 14 d after initiation of treatment. Tumors were fixed, paraffin embedded, sectioned and immunostained for CD31 or pEGFR, and counterstained with hematoxylin (CD31) or 4′,6-diamidino-2-phenylindole (pEGFR). Representative images at ×100 (CD31) and ×200 (pEGFR) for EXEL-7647 or erlotinib at 100 mg/kg show differential effect on pEGFR (*A-C*) and number of CD31-positive tumor vessels (*D-F*).

Table 3. Immunohistochemical analyses of EGFR phosphorylation and downstream effectors in H1975 xenograft tumors

Dose (mg/kg)	Tumor size		$pEGFR^{Tyr1068}$		$pERK^{Thr202/Tyr204}$		$pAKT^{Ser473}$	
	Mean (mg)	TGI (%)	% Cells	% Reduction	% Cells	% Reduction	% Cells	% Reduction
Vehicle	1,091 ± 61	NA	27 ± 1.8	NA	23 ± 2.6	NA	42 ± 2.0	NA
EXEL-7647 (10)	758 ± 51	33*	14 ± 1.9	49.0*	20 ± 4.3	11.8 ns	19 ± 2.1	53.6*
EXEL-7647 (30)	436 ± 54	66*	12 ± 1.3	56.1*	13 ± 4.9	41.8*	12 ± 1.9	72.4*
EXEL-7647 (100)	171 ± 15	92*	10 ± 1.8	63.7*	10 ± 3.7	57.1*	11 ± 1.9	74.4*
Erlotinib (30)	766 ± 66	33†	24 ± 1.6	11.0 ns	18 ± 6.0	20.5†	25 ± 1.6	39.0*
Erlotinib (100)	724 ± 68	37*	23 ± 1.6	16.1*	14 ± 5.0	38.8*	23 ± 1.9	45.3*

NOTE: Values are mean ± SD. Tumor growth inhibition versus vehicle control.
Abbreviations: TGI, tumor growth inhibition; NA, not applicable; ns, not significant.
*$P < 0.0001$.
†$P < 0.005$.

Discussion

Targeted therapies have recently attracted significant attention as anticancer agents. The most encouraging clinical results to date have been achieved in malignancies driven by mutationally activated kinases, including chronic myelogenous leukemia (Bcr-Abl), gastrointestinal stromal tumors (c-Kit), and a subset of NSCLC patients with mutationally activated EGFRs (9, 10, 33, 34). However, the currently approved therapies targeting cancers driven by such activating mutations are only impactful for a relatively small fraction of the cancer patient population. It has also become apparent that individuals who initially benefit from treatment with a selective kinase inhibitor (e.g., imatinib) may later become unresponsive due to the emergence of drug resistance mutations in the gene encoding the target kinase (34). The majority of cancer patients are therefore in need of more broadly active anticancer agents that will combine targeted potency against both WT and drug resistance mutations with tolerable side effect profiles. Here, we describe a novel spectrum-selective kinase inhibitor, EXEL-7647, that is a potent inhibitor of both EGFR and VEGFR family members and additionally inhibits EphB4. EXEL-7647 inhibits EGFR signaling in cells and retains significant activity against mutant EGFRs associated with resistance to erlotinib and gefitinib.

Members of the EGF RTK family (EGFR, ErbB2, ErbB3, and ErbB4) are overexpressed in many solid tumors. Several anti-EGFR therapies (gefitinib, erlotinib, and cetuximab) have been approved for the treatment of NSCLC or colorectal cancer, and the anti-ErbB2 antibody, trastuzumab, is approved for the treatment of ErbB2-positive breast cancers. EXEL-7647 inhibits the kinase activities and activation of both EGFR and ErbB2. Although patients who have EGFR kinase domain mutations respond to gefitinib and erlotinib, many develop resistance to these drugs over time. A recent study by Pao et al. (14) has defined the mechanism that underlies the acquired resistance observed in some of these patients. A "second site" mutation in EGFR results in a substitution of a methionine for a conserved threonine at residue 790 (T790M). This change is presumed to inhibit the ability of gefitinib or erlotinib to form a critical hydrogen bond within the ATP-binding pocket of the catalytic region (35). The acquisition of clinical resistance observed following treatment with small-molecule EGFR inhibitors in NSCLC is similar to that observed in chronic myelogenous leukemia and gastrointestinal stromal tumor subjects who relapse following treatment with imatinib (36, 37). The observation that inhibition of drug action can be accomplished by a similar mechanism in three different disease/treatment scenarios emphasizes the need for therapeutics that show efficacy against kinases harboring the gatekeeper mutation.

Table 4. Immunohistochemical analyses of apoptosis, tumor vessel density, and Ki67 index in H1975 xenograft tumors

Dose (mg/kg)	Tumor size		TUNEL		CD31 analysis		Ki67 analysis	
	Mean (mg)	TGI (%)	% Cells	Fold increase	MVC	% Reduction	% Cells	% Reduction
Vehicle	1,091 ± 61	NA	1 ± 0.2	NA	62 ± 8	NA	35 ± 3	NA
EXEL-7647 (10)	758 ± 51	33*	6 ± 0.8	7.1*	44 ± 10	30.0†	27 ± 4	23.2†
EXEL-7647 (30)	436 ± 54	66*	11 ± 1.4	11.9*	34 ± 9	46.1*	20 ± 5	41.9*
EXEL-7647 (100)	171 ± 15	92*	15 ± 1.8	16.5*	19 ± 11	69.6*	8.9 ± 2	74.6*
Erlotinib (30)	766 ± 66	33†	4 ± 1.0	4.5*	55 ± 7	11.0 ns	26 ± 5	25.6†
Erlotinib (100)	724 ± 68	37*	5 ± 1.1	5.1*	63 ± 8	0.0 ns	21 ± 4	40.9*

NOTE: Values are mean ± SD. Tumor growth inhibition versus vehicle control.
Abbreviations: TUNEL, terminal deoxynucleotidyl transferase–mediated dUTP nick end labeling; MVC, mean vessel count/mm^2.
*$P < 0.0001$.
†$P < 0.005$.

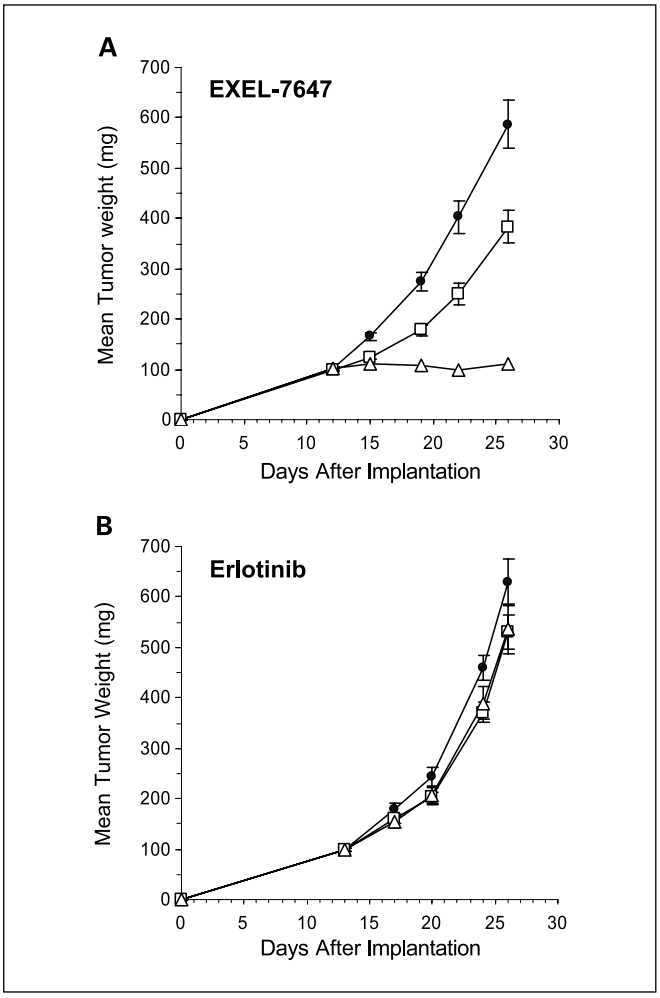

Fig. 5. Tumor growth inhibition of EXEL-7647 or erlotinib in MDA-MB-231 xenografts. Tumors were established following s.c. implantation into the mammary fat pad of nude mice, staged to 100 mg, and randomized into treatment groups ($n = 10$ per group). Oral administration of EXEL-7647, erlotinib, or vehicle was initiated and continued once daily for 14 d. Points, mean tumor size for 10 mice per treatment group; bars, SE. *A,* EXEL-7647 (□, 30 mg/kg/d; △, 100 mg/kg/d), vehicle (●). *B,* erlotinib (□, 30 mg/kg/d; △, 100 mg/kg), vehicle (●).

Our studies using the bronchoalveolar cell line H1975, which harbors the EGFR double mutation (L858R and T790M), provide a means to evaluate the ability of small molecules to inhibit activation of the gatekeeper EGFR mutant. EXEL-7647 inhibits cellular proliferation of H1975 with a IC_{50} value of 820 nmol/L, which is ~12 and 15 times more potent than gefitinib and erlotinib, respectively. Additionally, EXEL-7647 inhibits the phosphorylation of the double-mutant EGFR and the subsequent activation of downstream survival and proliferation pathways as measured by inhibition of phosphorylation of AKT and ERK, respectively. When H1975 cells were established as s.c. xenografts in severe combined immunodeficient mice, once-daily oral administration of EXEL-7647 resulted in strong, dose-dependent inhibition of tumor growth. In contrast, erlotinib showed only moderate efficacy. Immunohistochemical analysis of tumors at the end of the dosing period showed that EXEL-7647 inhibited the phosphorylation of EGFR and the downstream effectors AKT and ERK, consistent with inhibition of EGFR T790M *in vivo*. EXEL-7647 treatment also caused significant reductions in tumor vessel density, which is consistent with inhibition of VEGFRs. Tumors from EXEL-7647–treated animals also showed marked inhibition of cell proliferation and increases in apoptosis when compared with tumors from vehicle-treated animals. In contrast, tumors from erlotinib-treated animals showed no changes in tumor vessel density and modest changes in proliferation, apoptosis, pEGFR, pAKT, and pERK.

In addition to inhibition of EGFR, EXEL-7647 is also a potent inhibitor of VEGFRs; therefore, the effect of EXEL-7647 and erlotinib was examined in the MDA-MB-231 xenograft model that highly expresses VEGF (26, 27) and is less reliant on signaling through EGFR (28). Consistent with inhibition of both tumor growth and proangiogenic RTKs, EXEL-7647 was highly efficacious in this model, whereas erlotinib did not significantly inhibit tumor growth. Immunohistochemical analyses of tumors at the end of the study showed that EXEL-7647 caused a significant decrease in tumor vessel density (CD31) and tumor cell proliferation (Ki67) showing inhibitory effects of EXEL-7647 on both tumor cell growth and the tumor vasculature. In contrast, the selective EGFR inhibitor, erlotinib, had no effect on number of CD31-positive tumor vessels and showed a moderate but significant decrease in tumor cell proliferation. Given that human malignancy is a multifaceted disease, these data show the potential advantage of a small molecule that targets multiple RTKs associated with critical components of tumor pathobiology. This spectrum of potent inhibitory activities translates to increased and broader efficacy when compared with a selective agent.

Table 5. Immunohistochemical analyses of tumor vessel density and Ki67 index in MDA-MB-231 xenograft tumors

Dose (mg/kg)	Tumor size		CD31 analysis		Ki67 analysis	
	Mean (mg)	TGI (%)	MVC	% Reduction	% Cells	% Reduction
Vehicle	587 ± 49	NA	64 ± 10	NA	49 ± 10	NA
EXEL-7647 (30)	383 ± 33	41.9*	28 ± 10	55.5†	28 ± 10	42.6†
EXEL-7647 (100)	112 ± 5	97.6†	5 ± 5	91.8†	25 ± 5	49.6†
Vehicle	629 ± 47	NA	78 ± 10	NA	40 ± 5	NA
Erlotinib (30)	531 ± 35	18.6 ns	65 ± 20	16.6 ns	32 ± 4	21.9†
Erlotinib (100)	536 ± 50	17.4 ns	76 ± 7	3.3 ns*	32 ± 5	21.4†

NOTE: Values are mean ± SD. Tumor growth inhibition versus respective vehicle control.
*$P < 0.005$.
†$P < 0.0001$.

EXEL-7647 is an ATP competitive and reversible inhibitor of EGFR, ErbB2, EphB4, and KDR. A class of irreversible EGFR inhibitors has been described that also shows *in vitro* activity against the T790M mutation in cell lines (38, 39). However, because no *in vivo* studies have been described using these compounds, their effect on tumor growth in animal studies is currently unknown.

In summary, EXEL-7647 is a highly potent spectrum-selective kinase inhibitor of the clinically validated RTK EGFR and importantly retains inhibitory activity against the gatekeeper EGFR mutation that is resistant to EGFR inhibitors that are currently approved. In addition to inhibition of EGFR, EXEL-7647 also potently inhibits two other clinically validated RTKs ErbB2 and KDR as well as the proangiogenic EphB4. By simultaneously targeting multiple signal transduction pathways that are involved in tumor growth and angiogenesis, EXEL-7647 may have broader clinical utility than agents with more restricted specificity profiles.

Acknowledgments

We thank Dr. Abhijit Guha for generously providing the Tet-On inducible EGFR and EGFRvIII expression constructs, Bristol-Myers Squibb Oncology for Lx-1 cells, and numerous members of the Exelixis Drug Discovery and Translational Medicine Departments for their support.

References

1. Krause DS, Van Etten RA. Tyrosine kinases as targets for cancer therapy. N Engl J Med 2005;353:172–87.
2. Medinger M, Drevs J. Receptor tyrosine kinases and anticancer therapy. Curr Pharm Des 2005;11:1139–49.
3. Mendelsohn J, Baselga J. The EGF receptor family as targets for cancer therapy. Oncogene 2000;19:6550–65.
4. Spano JP, Fagard R, Soria JC, et al. Epidermal growth factor receptor signaling in colorectal cancer: preclinical data and therapeutic perspectives. Ann Oncol 2005;16:189–94.
5. Guy PM, Platko JV, Cantley LC, Cerione RA, Carraway KL III. Insect cell-expressed p180erbB3 possesses an impaired tyrosine kinase activity. Proc Natl Acad Sci U S A 1994;91:8132–6.
6. Kim HH, Vijapurkar U, Hellyer NJ, Bravo D, Koland JG. Signal transduction by epidermal growth factor and heregulin via the kinase-deficient ErbB3 protein. Biochem J 1998;334:189–95.
7. Grant S, Qiao L, Dent P. Roles of ERBB family receptor tyrosine kinases, and downstream signaling pathways, in the control of cell growth and survival. Front Biosci 2002;7:d376–89.
8. Ciardiello F, Tortora G. A novel approach in the treatment of cancer: targeting the epidermal growth factor receptor. Clin Cancer Res 2001;7:2958–70.
9. Lynch TJ, Bell DW, Sordella R, et al. Activating mutations in the epidermal growth factor receptor underlying responsiveness of non-small-cell lung cancer to gefitinib. N Engl J Med 2004;350:2129–39.
10. Paez JG, Janne PA, Lee JC, et al. EGFR mutations in lung cancer: correlation with clinical response to gefitinib therapy. Science 2004;304:1497–500.
11. Pedersen MW, Meltorn M, Damstrup L, Poulsen HS. The type III epidermal growth factor receptor mutation. Biological significance and potential target for anti-cancer therapy. Ann Oncol 2001;12:745–60.
12. Batra SK, Castelino-Prabhu S, Wikstrand CJ, et al. Epidermal growth factor ligand-independent, unregulated, cell-transforming potential of a naturally occurring human mutant EGFRvIII gene. Cell Growth Differ 1995;6:1251–9.
13. Amann J, Kalyankrishna S, Massion PP, et al. Aberrant epidermal growth factor receptor signaling and enhanced sensitivity to EGFR inhibitors in lung cancer. Cancer Res 2005;65:226–35.
14. Pao W, Miller VA, Politi KA, et al. Acquired resistance of lung adenocarcinomas to gefitinib or erlotinib is associated with a second mutation in the EGFR kinase domain. PLoS Med 2005;2:e73.
15. Hicklin DJ, Ellis LM. Role of the vascular endothelial growth factor pathway in tumor growth and angiogenesis. J Clin Oncol 2005;23:1011–27.
16. Mercurio AM, Bachelder RE, Bates RC, Chung J. Autocrine signaling in carcinoma: VEGF and the $\alpha_6\beta_4$ integrin. Semin Cancer Biol 2004;14:115–22.
17. Brantley-Sieders D, Parker M, Chen J. Eph receptor tyrosine kinases in tumor and tumor microenvironment. Curr Pharm Des 2004;10:3431–42.
18. Liu W, Jung YD, Ahmad SA, et al. Effects of overexpression of ephrin-B2 on tumour growth in human colorectal cancer. Br J Cancer 2004;90:1620–6.
19. Dobrzanski P, Hunter K, Jones-Bolin S, et al. Antiangiogenic and antitumor efficacy of EphA2 receptor antagonist. Cancer Res 2004;64:910–9.
20. Carles-Kinch K, Kilpatrick KE, Stewart JC, Kinch MS. Antibody targeting of the EphA2 tyrosine kinase inhibits malignant cell behavior. Cancer Res 2002;62:2840–7.
21. Xia G, Kumar SR, Masood R, et al. EphB4 expression and biological significance in prostate cancer. Cancer Res 2005;65:4623–32.
22. Nakamoto M, Bergemann AD. Diverse roles for the Eph family of receptor tyrosine kinases in carcinogenesis. Microsc Res Tech 2002;59:58–67.
23. Dodelet VC, Pasquale EB. Eph receptors and ephrin ligands: embryogenesis to tumorigenesis. Oncogene 2000;19:5614–9.
24. Sini P, Wyder L, Schnell C, et al. The antitumor and antiangiogenic activity of vascular endothelial growth factor receptor inhibition is potentiated by ErbB1 blockade. Clin Cancer Res 2005;15:4521–32.
25. Chan CT, Metz MZ, Kane SE. Differential sensitivities of trastuzumab (Herceptin)-resistant human breast cancer cells to phosphoinositide-3 kinase (PI-3K) and epidermal growth factor receptor (EGFR) kinase inhibitors. Breast Cancer Res Treat 2005;91:187–201.
26. Franco M, Man S, Chen L, et al. Targeted anti-vascular endothelial growth factor receptor-2 therapy leads to short-term and long-term impairment of vascular function and increase in tumor hypoxia. Cancer Res 2006;66:3639–48.
27. Chelouche-Lev D, Miller CP, Tellez C, et al. Different signalling pathways regulate VEGF and IL-8 expression in breast cancer: implications for therapy. Eur J Cancer 2004;40:2509–18.
28. Fan WH, Lu YL, Deng F, et al. EGFR antisense RNA blocks expression of the epidermal growth factor receptor and partially reverse the malignant phenotype of human breast cancer MDA-MB-231 cells. Cell Res 1998;8:63–71.
29. Rice KD, Anand NK, Bussenius J, et al. Receptor-type kinase modulators and methods of use. United States patent WO2004006846. 2004 Jan 22.
30. Barker AJ, Gibson KH, Grundy W, et al. Studies leading to the identification of ZD1839 (IRESSA): an orally active, selective epidermal growth factor receptor tyrosine kinase inhibitor targeted to the treatment of cancer. Bioorg Med Chem Lett 2001;11:1911–4.
31. Schnur RC, Arnold LD. Preparation of *N*-phenylquinazoline-4-amines as neoplasm inhibitors. United States patent WO9630347. 1996 Oct. 03.
32. Reiss M, Stash EB, Vellucci VF, Zhou ZL. Activation of the autocrine transforming growth factor α pathway in human squamous carcinoma cells. Cancer Res 1991;51:6254–62.
33. Klapper LN, Waterman H, Sela M, Yarden Y. Tumor-inhibitory antibodies to HER-2/ErbB-2 may act by recruiting c-Cbl and enhancing ubiquitination of HER-2. Cancer Res 2000;60:3384–8.
34. Chen LL, Trent JC, Wu EF, et al. A missense mutation in KIT kinase domain 1 correlates with imatinib resistance in gastrointestinal stromal tumors. Cancer Res 2004;64:5913–9.
35. Stamos J, Sliwkowski MX, Eigenbrot C. Structure of the epidermal growth factor receptor kinase domain alone and in complex with a 4-anilinoquinazoline inhibitor. J Biol Chem 2002;277:46265–72.
36. Gorre ME, Mohammed M, Ellwood K, et al. Clinical resistance to STI-571 cancer therapy caused by BCR-ABL gene mutation or amplification. Science 2001;293:876–80.
37. Shah NP, Tran C, Lee FY, et al. Overriding imatinib resistance with a novel ABL kinase inhibitor. Science 2004;305:399–401.
38. Kobayashi S, Ji H, Yuza Y, et al. An alternative inhibitor overcomes resistance caused by a mutation of the epidermal growth factor receptor. Cancer Res 2005;65:7096–101.
39. Kwak EL, Sordella R, Bell DW, et al. Irreversible inhibitors of the EGF receptor may circumvent acquired resistance to gefitinib. Proc Natl Acad Sci U S A 2005;102:7665–70.